Relevance of radiator installation on the efficacy of noise reduction strategies in an industrial engine cooling fan

DOI: 10.61782/fa.2025.0742

FORUM ACUSTICUM
EURONOISE 2025

RELEVANCE OF RADIATOR INSTALLATION ON THE EFFICACY OF NOISE REDUCTION STRATEGIES IN AN INDUSTRIAL ENGINE COOLING FAN

Francesco Bellelli* **Renzo Arina** **Francesco Avallone**
Department of Mechanical and Aerospace Engineering, Politecnico di Torino, Torino, Italy

ABSTRACT

Engine cooling fans must be efficient and quieter, as their acoustic contribution is today more noticeable considering the reduced noise from electric motors. Therefore, more effective noise reduction technologies must be designed. This paper investigates how noise reduction technologies, designed for an isolated fan, are impacted by the presence of a radiator pulling upstream. Two modifications to the baseline fan geometry are studied: (i) one with a ring shape that mitigates the backflow-rotor interaction and (ii) one with stator vane azimuthal spacing optimized to reduce rotor-stator interaction tonal noise. They are assessed with high-fidelity simulations performed both on an isolated fan and a full cooling module including the radiator, which is simulated using an equivalent porous medium. Results reveal that the modified ring shape effectively prevents backflow-rotor interaction on the isolated fan, reducing broadband noise by radially redirecting the backflow. However, its performance is less effective when a radiator is present due to the presence of the casing. Conversely, stator vane optimized spacing shows robust noise reduction in both configurations, because the effect of distributing tonal energy across several modes is not altered by the presence of the radiator.

Keywords: *Radiator, installation, fan, noise sources, noise reduction*

**Corresponding author*: *francesco.bellelli@polito.it.*

1. INTRODUCTION

With the transition to electric motors, reducing car component noise emissions has become a critical focus. This shift has led the scientific community to investigate several conventional [1] and bio-inspired [2] noise reduction strategies.

One of the main noise contribution for low-speed fans is tip-clearance noise, generated by coherent vortex structures present in the tip-gap region [3]. Tip-clearance noise is usually mitigated by introducing a rotating ring [4] to prevent the formation and growth of coherent structures responsible for sub-harmonic humps. However, a rotating ring may generate unwanted flow patterns if the fan is subjected to a pressure rise, causing backflow end increasing unsteady loading noise. It has been demonstrated that rotor-backflow interaction is a major source of unsteady loading noise even at design conditions [5, 6]. Strategies such as tailored short ducts [7], porous leading edges [8], or serrated bio-inspired designs [9] have been conceived to mitigate this noise source, albeit they increase high-frequency broadband noise.

Rotor-stator interaction is another significant noise source [10] for fans. If the rotor-stator axial clearance is short, aerodynamic potential effect dominates over wake impingement [11]. Geometrical azimuthal inhomogeneities might increase noise [12] and give rise to additional azimuthal pressure modes. Unevenly spacing the vanes with specific modulations, as done by Duncan [13] and Mellin-Sovran [14], is a typical solution. However, these approaches act only in a discrete fashion on the vanes spacing, eventually discarding optimal solutions, as repoted in Ref. [15].

A comprehensive understanding of how these strategies influence backflow-rotor interactions still deserves

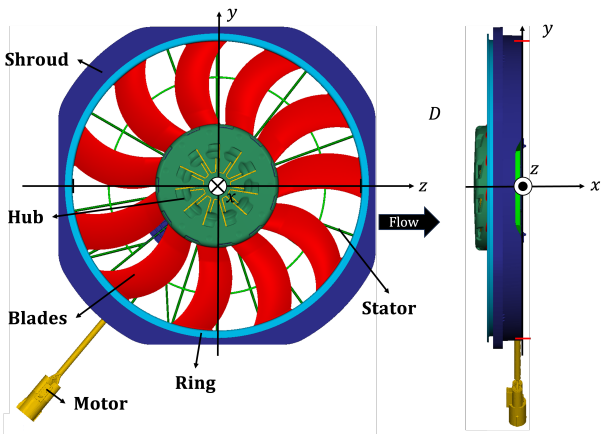

Figure 1: Tested automotive engine fan. The main parts in which the fan consists are shown with different colors.

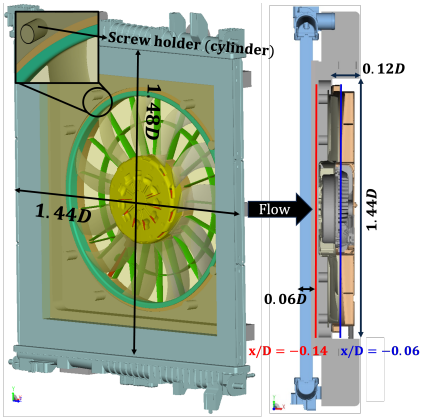

Figure 2: Tested radiator. The heat exchanger is shown in light blue (solid part) and yellow (coolant tubes part), while the square casing is shown in grey.

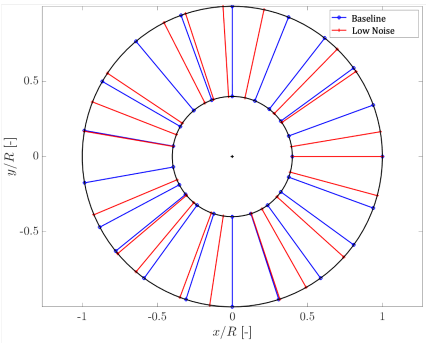

Figure 3: Baseline and low-noise stator-vane azimuthal distributions.

further studies. Deterministic unsteady loading contributions such as non-viscous rotor-stator interaction are rarely addressed, and optimization procedures to mitigate these effects are almost absent. Finally, most noise reduction techniques are evaluated on isolated fans rather than on the real installed configuration. This must be considered when the same casing, for the fan and the radiator, is used to test different configurations [16]. This aspect is expected to impact the efficacy of noise reduction techniques when applied to a baseline fan.

This paper examines numerically the influence of shape modifications of the rotating ring to mitigate the backflow-rotor interaction noise and explores the effects of stator-vane uneven spacing to minimize rotor-stator interaction tonal noise. Furthermore, the paper considers how the radiator installation impacts the performance of noise reduction strategies in typical operations.

2. FAN AND RADIATOR GEOMETRY

The fan consists of a 465 mm diameter (D) rotor with $B = 11$ unevenly spaced blades connected to a ring, a hub, a driving electrical motor, $N_v = 20$ unevenly spaced stator-vane, and a shroud, as shown in Fig. 1. The fan tip-clearance is equal to $0.009D$. The radiator consists of a heat exchanger of $1.44D \times 1.48D$ placed $0.02D$ upstream of the fan hub and of a square casing that joins it to the fan, as shown in Fig. 2.

A first modification to the ring geometry was performed with the scope of preventing the backflow to interact with the blades. The ring shape was modified to further redirect the backflow from the blades. The axial spacing between the ring and stator-vane was reduced by 30% to mitigate adverse flow in the tip-clearance. The shroud was shifted forward in the x direction of the top structure to keep constant the axial spacing with respect to the ring.

A second modification concerned the stator vane azimuthal distribution. The spacing was designed following the random spacing approach as described in Ref. [15]. This allows to redistribute more efficiently the acoustic energy of the rotor-stator interaction tones. In Fig. 3 the baseline and low-noise stator-vane azimuthal distributions are represented.

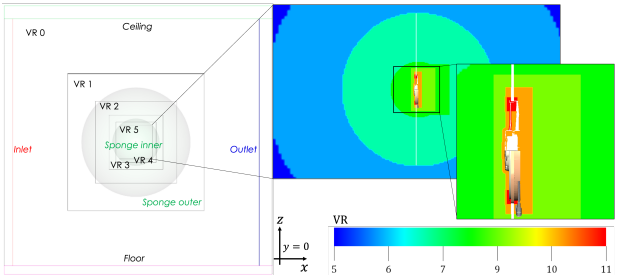

Figure 4: Sketch of the computational domain in the plane at $y/D = 0$.

3. NUMERICAL SETUP

Simulations have been performed with the commercial software 3DS PowerFLOW version 6, based on the lattice-Boltzmann method (LBM) [17].

The computational domain used to simulate all the configurations is shown in Fig. 4. A large fluid domain of $135D \times 135D \times 135D$ was built to simulate a free-field environment that encloses the fan. The ceiling and the floor of the simulation domain were modelled as a solid reflecting wall, while both inlet and outlet had a static ambient pressure boundary condition. A discretization strategy based on 11 Variable Resolution (VR) regions was adopted. The regions with maximum resolutions were set around the rotating blades and near the tip gap region, where there are 11 voxels in the tip-clearance. The resolution in the tip gap region was similar to the one adopted by Avallone et al. [18]. The voxel size between one VR region and the adjacent one was doubled. In the VR3 region, a sponge region was defined by an artificial change of viscosity of a factor of 100, with an exponential function between the inner and outer region, as outlined in Fig. 4. Both the increase in voxel size and the sponge region were used to mitigate reflections of acoustics waves at the domain boundaries.

In the isolated fan configuration, an anechoic wall separating the two environments was introduced so that a pressure rise Δp across the fan could be imposed [6]. The fan maximum efficiency point was simulated, corresponding to a load coefficient of $\psi = \frac{\Delta p}{\frac{1}{2}\rho v_{tip}^2} = 0.14$, where ρ is the ambient density and v_{tip} is the tip velocity, and a flow coefficient of $\varphi = \frac{\dot{V}}{\pi(R_{tip}^2 - R_{hub}^2)v_{tip}} = 0.10$, where $\dot{V}$ is the volume flow rate through the fan. R_{tip} and R_{hub} are respectively the tip and hub radii. In the full cooling module configuration, the heat exchanger was modelled as an equivalent porous medium [19]. No pressure difference was imposed in this configuration, as the equivalent porous medium provided the fan with a pressure loss which corresponded roughly to the maximum efficiency point of the complete cooling module system.

A physical time of 20 revolutions was simulated at a resolution of 1200 voxel per diameter (vox/D) in the finest VR region. A grid resolution study was performed on this setup in a previous work [6]. Data was saved only during the last 10 revolutions. Two planes parallel to the fan were sampled at $x/D = -0.14$ and $x/D = -0.06$ to compute averaged flow fields. The locations correspond respectively to the rotating ring upstream boundary and the rotor-stator interstage. Pressure on all the solid surfaces of the cooling module was sampled at a frequency of $48,000\,Hz$ and the volume flow rate was sampled, at the same frequency, on a plane at $x = 0/D$. Finally, a fully circular array of 12 equally spaced far-field probes, located in the plane $z/D = 0$ at a radius $r/D = 2.15$ far from the fan centre, was used to sample directly the acoustic field from the simulations. The spectral content of the signals was computed through the Welch averaging algorithm [20] with 8 Hamming windows and 50% of overlap, resulting in a frequency resolution of $11.8\,Hz$.

4. RESULTS

4.1 Isolated fan

ΔT [%]	$\Delta \dot{V}$ [%]	ΔQ [%]	$\Delta \eta$ [%]
+2.0	+6.4	+10.9	-6.0

Table 1: Aerodynamic performance variation between the baseline and low-noise geometries in the isolated fan configurations.

First, the effects of the proposed noise reduction strategies on the aerodynamic performance is discussed. In Tab. 1 the variations of axial thrust force (T), volume flow rate through the fan ($\dot{V}$), aerodynamic torque (Q), and aerodynamic efficienc of the low-noise geometry with respect to the baseline geometry are reported. The efficiency is calculated as

$$\eta = \frac{\frac{T}{\pi(R_{tip}^2 - R_{hub}^2)}\dot{V}}{Q\Omega}, \tag{1}$$

where Ω is the fan rotational speed in rad/s. The low-noise configuration displays an increase of both thrust and

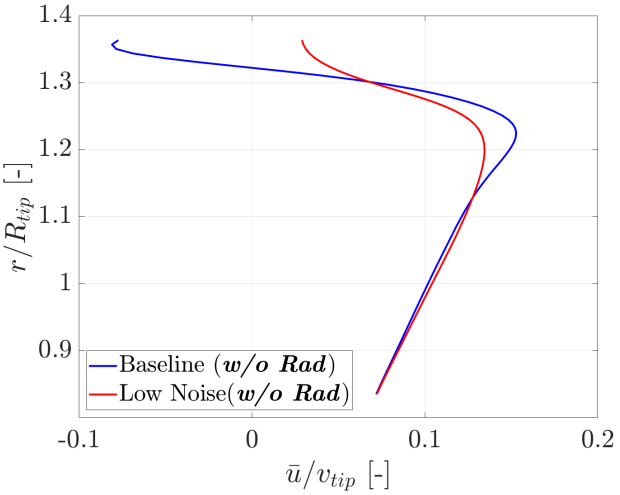

Figure 5: Mean axial velocity in the near-tip region ($0.8 \leq r/R_{tip} \leq 1.1$), at $x/D = -0.14$, azimuthally averaged.

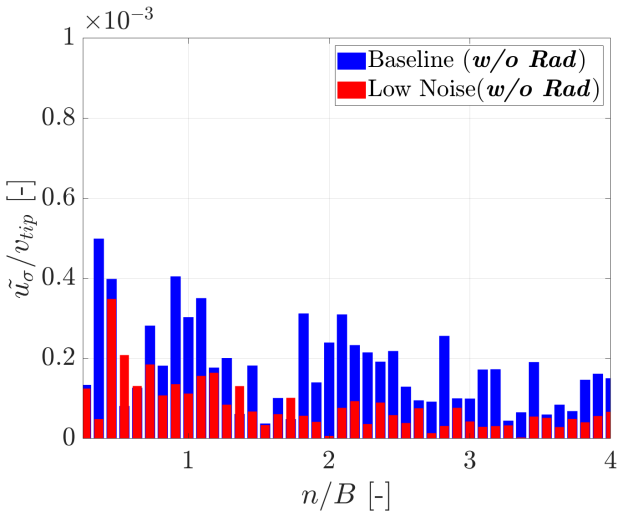

Figure 6: Azimuthal mode decomposition of the axial velocity root mean square (rms) sampled on a fully circular line at $r/R_{tip} = 0.9$ in a plane located at $x/D = -0.14$. n is the mode order and B is the number of rotor blades.

torque due to the increase of aerodynamic surface, as well as an increase of volume flow rate through the fan that can be explained with a decrease in backflow. However, both the increase in thrust and flow rate cannot compensate the increase in torque, leading to an aerodynamic efficiency reduction.

The impact of the ring shape on the upstream flow is analyzed. In Fig. 5 the time and azimuthally averaged axial velocity sampled on a plane at $x/D = -0.14$ is shown. The velocity is made dimensionless with the tip velocity. It is observed that the low-noise configuration reduces the velocity gradient in the region $1.1 \leq r/R_{tip} \leq 1.4$; $\bar{u}/v_{tip}$ does not attain negative values on the low-noise configuration, proving absence of the backflow.

The azimuthal mode decomposition of the axial velocity root mean square is shown in Fig. 6. The quantity is sampled on a plane at $x/D = -0.14$ and along a circular line at $r/R_{tip} = 0.9$. Results confirm previous observations, as the low-noise configuration is characterized by a considerable decrease in the axial velocity modal content among all the frequencies of interest. This is associated with the redirection of the backflow achieved by the modified ring geometry, reducing blade-backflow interaction.

The relevance of stator-vane azimuthal distribution is now discussed by looking at the azimuthal mode decomposition of the mean axial velocity in Fig. 7. The velocity is sampled on a plane at $x/D = -0.06$, which cor-

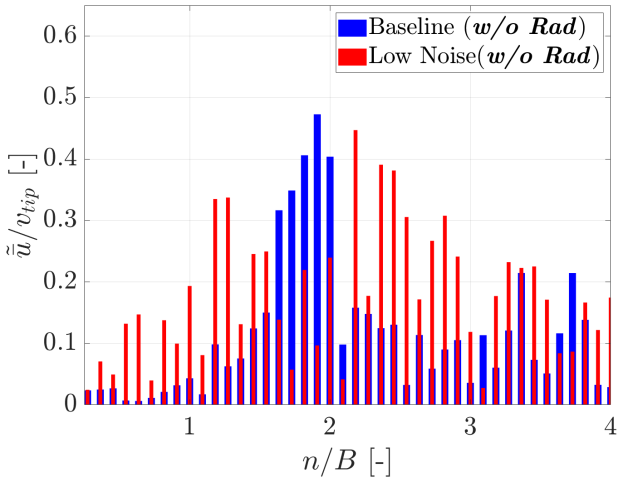

Figure 7: Azimuthal mode decomposition of the mean axial velocity sampled on a fully circular line at $r/R_{tip} = 0.7$ in a plane located at $x/D = -0.06$.

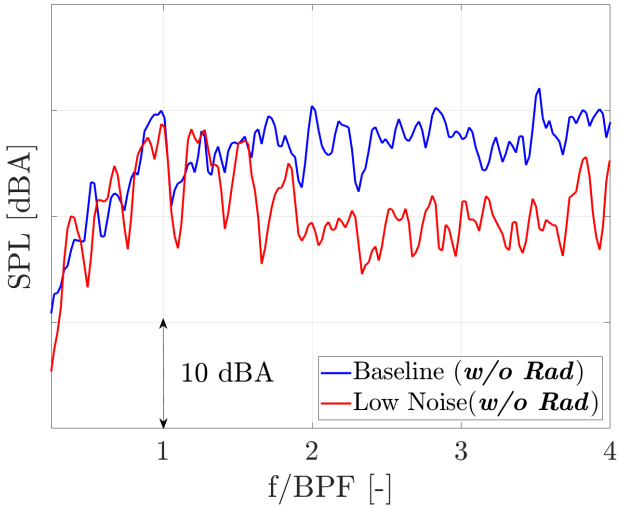

Figure 8: Pressure fluctuations at $x/D = -2.15$, $y/D = 0$, and $z/D = 0$.

responds to the rotor-stator interstage, and on a circular line located at $r/R_{tip} = 0.7$. The low-noise configuration positively contributes to the redistribution of energy among several other modes n. In particular, the low-noise configuration can substantially reduce the modal content in the range $1.5 \leq n/B \leq 2$, which has been previously shown by the authors [6] to be critically dominated by aerodynamic potential rotor-stator interaction on this fan configuration.

Finally, the efficacy of the proposed noise reduction strategies is discussed in Fig. 8, where the spectra of sound pressure fluctuations sampled at $x/D = -2.15$, $y/D = 0$, and $z/D = 0$ are shown in terms of Sound Pressure Level (SPL). The probe lies on the fan rotational axis, at a distance of $2.15D$ upstream of the fan. The frequency axis is made dimensionless with the blade passing frequency ($BPF = \omega B$, where ω is the fan rotational frequency in Hz). The spectrum clearly shows that the low-noise configuration is characterized by a considerable decrease in broadband content for $f/BPF \geq 1.5$. This improvement is attributed to the absence of backflow-rotor interaction in the low-noise configuration, achieved through the modified ring shape that redirects the backflow far from the blades. Moreover, it should be noted that also the tonal content of the low-noise configuration is reduced, especially in the range $1.5 \leq f/BPF \leq 2$, as a result of the optimized vane distribution. Both noise reduction strategies led to a decrease in Overall Sound Pressure Level (OASPL) of about $4.9\,dBA$.

ΔT [%]	$\Delta \dot{V}$ [%]	ΔQ [%]	$\Delta \eta$ [%]
-0.4	-2.6	+2.9	-5.7

Table 2: Aerodynamic performance variation between the baseline and low-noise geometries in the full cooling module configurations.

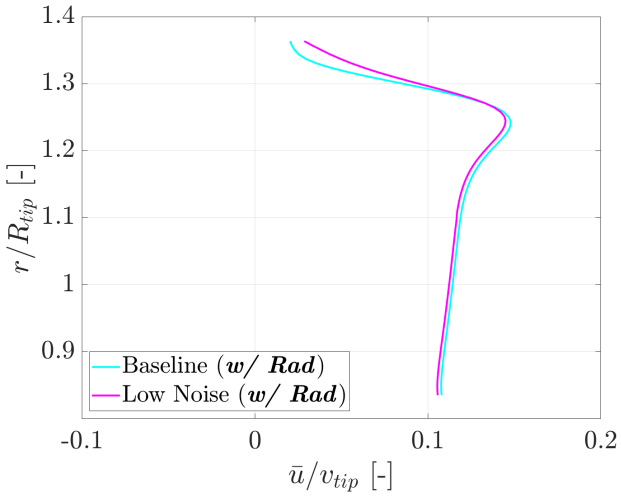

Figure 9: Mean axial velocity in the near-tip region ($0.8 \leq r/R_{tip} \leq 1.1$), at $x/D = -0.14$, azimuthally averaged.

4.2 Full cooling module

The variations in aerodynamic performance for the full cooling module baseline and low-noise configurations is assessed in Tab. 2. Overall, the low-noise geometry results in smaller variations of almost every investigated quantity. The thrust is mainly unaltered and the torque is only slightly increased. However, the volume flow rate through the fan is decreased, unlike the isolated fan configurations. This is due to a different flow physics associated with the backflow when considering the radiator installation. These differences in aerodynamic quantities lead to an aerodynamic efficiency decrease less important than the one for the isolated fan configurations (Tab. 1).

In Fig. 9 the time and azimuthally averaged axial velocity sampled on a plane at $x/D = -0.14$ is shown for the full cooling module configurations. The baseline and low-noise configurations have an almost identical spanwise trend of mean axial velocity near the tip, with a sub-

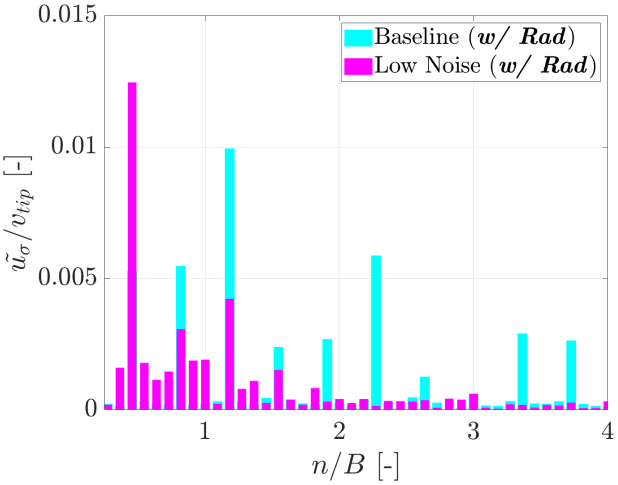

Figure 10: Azimuthal mode decomposition of the axial velocity root mean square (rms) sampled on a fully circular line at $r/R_{tip} = 0.9$ in a plane located at $x/D = -0.14$.

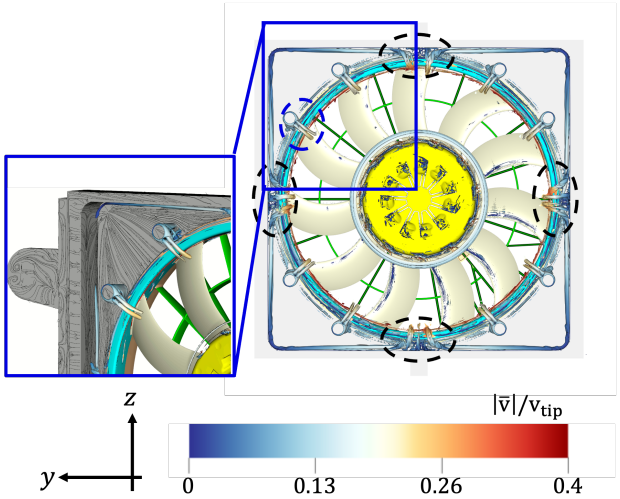

Figure 11: Mean $\Lambda_2 = -2.5 \cdot 10^5 1/s$ iso-surfaces coloured with velocity magnitude in the upstream casing for the baseline configurations.

stantial reduction of the mean axial velocity gradient with respect to the isolated fan, as seen in Fig. 5. This is associated with the presence of the equivalent porous medium, that has been previously shown by the authors [21] to locate the pressure losses on the fan disk up to $r/R_{tip} \leq 0.9$.

The azimuthal mode decomposition of the axial velocity root mean square at $x/D = -0.14$ and $r/R_{tip} = 0.9$ is shown in Fig. 10. It is observed an increase in the low frequency modal content up to $n/B \leq 2$ which is associated with the highly limited space in the radial extent due to the presence of the casing. This prevents the backflow to be radially redirected. Conversely, a stronger recirculation takes place in the casing upstream of the fan and is expected to negatively influence the acoustic performance of the system. The highly tonal content observed in both the baseline and low-noise configurations is instead associated with periodic recirculation spot in the casing that are due to the flow distortion induced by the square-to-round shape transition from the casing to the fan and by the presence of several cylindrical screw holders that are present in the casing. These features in the flow field are outlined for the baseline configuration only in Fig. 11, where $\Lambda_2 = -2.5 \cdot 10^5 1/s$ iso-surfaces are shown, colored by velocity magnitude.

In Fig. 12 the azimuthal mode decomposition of the mean axial velocity at $x/D = -0.06$ and r/R_{tip} shows that the stator-vane distribution is consistently able

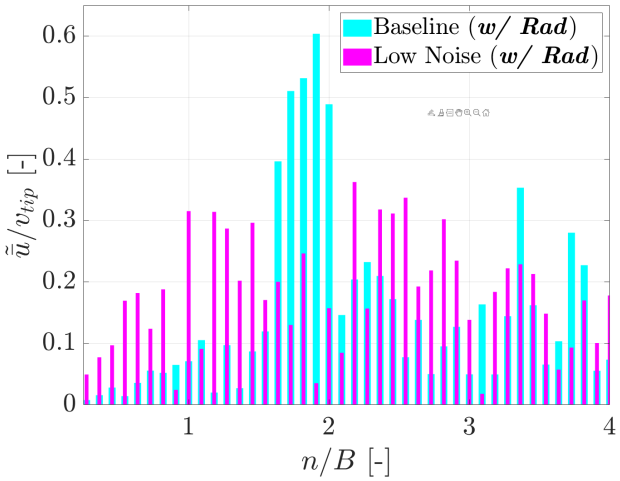

Figure 12: Azimuthal mode decomposition of the mean axial velocity sampled on a fully circular line at $r/R_{tip} = 0.7$ in a plane located at $x/D = -0.06$.

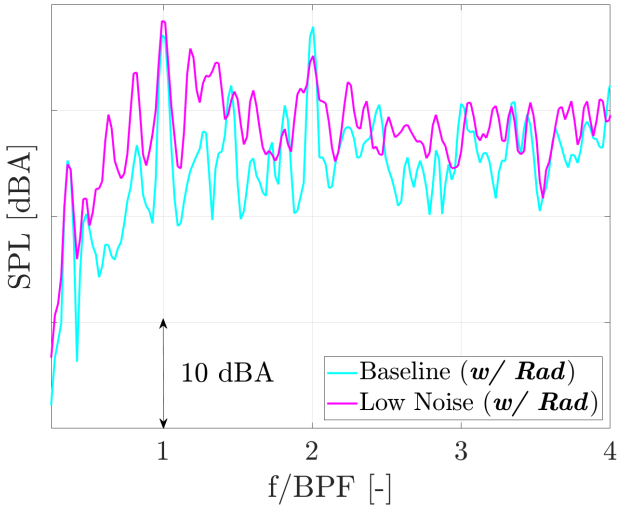

Figure 13: Pressure fluctuations at $x/D = -2.15$, $y/D = 0$, and $z/D = 0$.

to reduce the prominence of single modes n by heterogeneously distribute the energy, as seen also in Fig. 7 for the isolated fan configurations. As a matter of fact, the radiator installation does not influence the flow physics in the interstage between rotor and stator, leading to considerably similar results between the isolated fan and the full cooling module configurations.

In Fig. 13 the spectra of sound pressure fluctuations sampled at $x/D = -2.15$, $y/D = 0$, and $z/D = 0$ are shown. The probe location is upstream of both the fan and the radiator. The low frequency ($0.5 \leq f/BPF \leq 2$) broadband content of the low-noise configuration is higher than the baseline configuration, meaning that the modification on the ring shape is not consistently able to reduce the backflow-rotor interaction noise contribution. This results in a higher noise contribution in the low frequency range. From $f/BPF \geq 2$ the broadband content is similar to the baseline configuration. Nevertheless, the tonal content of the low-noise configuration is consistently lower than the baseline configuration, as a result of the stator-vane redistribution. It has been shown in Fig. 12 that the vanes are not influenced by the presence of the upstream radiator. The OASPL is increased by $2.5\,dBA$ because of the broadband content increase.

5. CONCLUSIONS

Two modifications to the baseline geometry of an engine cooling fan are studied: one with a ring shape that mitigates the backflow-rotor interaction and one with stator vane's spacing optimized to reduce rotor-stator interaction tonal noise. They are investigated on an isolated fan and a full module where the radiator is simulated as an equivalent porous medium. Results revealed that the proposed noise reduction strategies slightly reduced the aerodynamic performance, mainly because of the increased aerodynamic surface of the modified ring shape that led to a drastic increase in torque. The low-noise ring prevented backflow-rotor interaction on the isolated fan, but showed poor performance when the radiator is present because of its casing. On the other hand, stator vane spacing showed robust noise reduction in both configurations since the effect of distributing tonal energy across several modes is not altered by the presence of the radiator upstream. Results shown in this paper highlight the importance of considering the radiator installation when designing possible noise reduction strategies, especially when the flow physics exploited to reduce noise can be substantially altered by the presence of the radiator.

6. REFERENCES

[1] M. Piwowarski and D. Jakowski, "Areas of Fan Research—A Review of the Literature in Terms of Improving Operating Efficiency and Reducing Noise Emissions," *Energies*, vol. 16, p. 1042, Jan. 2023.

[2] W. Zhou, P. Zhou, C. Xiang, Y. Wang, J. Mou, and J. Cui, "A Review of Bionic Structures in Control of Aerodynamic Noise of Centrifugal Fans," *Energies*, vol. 16, p. 4331, May 2023.

[3] T. Zhu, D. Lallier-Daniels, M. Sanjosé, S. Moreau, and T. Carolus, "Rotating coherent flow structures as a source for narrowband tip clearance noise from axial fans," *Journal of Sound and Vibration*, vol. 417, pp. 198–215, Mar. 2018.

[4] F. Han, X. Chen, Y. Yang, and C. Wang, "Numerical and Experimental Study on the Effect of Rotor–Stator Distance on Rotor–Stator Interaction Strength within Mixed-Flow Centrifugal Pumps," *Journal of Marine Science and Engineering*, vol. 10, p. 1114, Aug. 2022.

[5] S. Magne, S. Moreau, and A. Berry, "Subharmonic tonal noise from backflow vortices radiated by a low-speed ring fan in uniform inlet flow," *The Journal of*

the Acoustical Society of America, vol. 137, pp. 228–237, Jan. 2015.

[6] F. Bellelli, R. Arina, and F. Avallone, "On the impact of operating condition and testing environment on the noise sources in an industrial engine cooling fan," *Applied Acoustics*, vol. 227, p. 110252, Jan. 2025.

[7] Z. Sun, J. Tian, T. Zhang, Z. Du, and H. Ouyang, "Cooling fan aerodynamic noise reduction with short inlet duct and its applicability," *International Journal of Refrigeration*, vol. 148, pp. 117–130, Apr. 2023.

[8] C. Teruna, L. Rego, D. Casalino, D. Ragni, and F. Avallone, "A Numerical Study on Aircraft Noise Mitigation Using Porous Stator Concepts," *Aerospace*, vol. 9, p. 70, Jan. 2022.

[9] Z. Liang, J. Wang, W. Wang, B. Jiang, Y. Ding, and W. Qin, "Numerical and Experimental Investigations of Axial Flow Fan with Bionic Forked Trailing Edge," *Machines*, vol. 11, p. 155, Jan. 2023.

[10] J. M. Tyler and T. G. Sofrin, "Axial Flow Compressor Noise Studies," in *Pre-1964 SAE Technical Papers*, vol. Pre-1964 SAE Technical Papers, p. 620532, Jan. 1962.

[11] E. Canepa, A. Cattanei, and F. Mazzocut Zecchin, "Effect of the rotor–stator gap variation on the tonal noise generated by axial-flow fans," *Applied Acoustics*, vol. 94, pp. 29–38, July 2015.

[12] M. Pestana, M. Sanjosé, S. Moreau, M. Roger, and M. Gruber, "Investigation on the noise of an axial low mach-number fan stage with a heterogeneous stator," *FAN 2018*, 2018.

[13] P. Duncan and B. Dawson, "Reduction of interaction tones from axial flow fans by suitable design of rotor configuration," *Journal of Sound and Vibration*, vol. 33, pp. 143–154, Mar. 1974.

[14] R. C. Mellin and G. Sovran, "Controlling the Tonal Characteristics of the Aerodynamic Noise Generated by Fan Rotors," *Journal of Basic Engineering*, vol. 92, pp. 143–154, Mar. 1970.

[15] A. Cattanei, F. Mazzocut Zecchin, A. Di Pasquali, and A. Lazari, "Effect of the uneven blade spacing on the noise annoyance of axial-flow fans and side channel blowers," *Applied Acoustics*, vol. 177, p. 107924, June 2021.

[16] M. Sortor, "On-System Engine Cooling Fan Measurement as a Tool for Optimizing Cooling System Airflow Performance and Noise," *SAE International Journal of Materials and Manufacturing*, vol. 4, pp. 1221–1230, Apr. 2011.

[17] X. He and L.-S. Luo, "Theory of the lattice Boltzmann method: From the Boltzmann equation to the lattice Boltzmann equation," *Physical Review E*, vol. 56, pp. 6811–6817, Dec. 1997.

[18] F. Avallone, D. Ragni, and D. Casalino, "On the effect of the tip-clearance ratio on the aeroacoustics of a diffuser-augmented wind turbine," *Renewable Energy*, vol. 152, pp. 1317–1327, June 2020.

[19] M. Piellard, B. B. Coutty, V. Le Goff, V. Vidal, and F. Perot, "Direct aeroacoustics simulation of automotive engine cooling fan system: effect of upstream geometry on broadband noise," in *20th AIAA/CEAS Aeroacoustics Conference*, (Atlanta, GA), American Institute of Aeronautics and Astronautics, June 2014.

[20] P. Welch, "The use of fast Fourier transform for the estimation of power spectra: A method based on time averaging over short, modified periodograms," *IEEE Transactions on Audio and Electroacoustics*, vol. 15, pp. 70–73, June 1967.

[21] F. Bellelli, R. Arina, S. Moreau, and F. Avallone, "Aeroacoustics analysis of radiator installation effects in a pulling engine cooling module," in *FAN2025 Conference*, FAN2025 Conference, Apr. 2025.